Received: 2 November 2021 | Revised: 17 February 2022 | Accepted: 16 March 2022

DOI: 10.1002/jemt.24115

REVIEW ARTICLE

MICROSCOPY RESEARCH & TECHNIQUE WILEY

Detection and identification of coronaviruses in human tissues using electron microscopy

Hannah A. Bullock[1,2] | Cynthia S. Goldsmith[2] | Sara E. Miller[3]

[1]Synergy America, Inc., Atlanta, Georgia, USA

[2]Centers for Disease Control and Prevention, Atlanta, Georgia, USA

[3]Duke Medical Center, Durham, North Carolina, USA

Correspondence
Hannah A. Bullock, Centers for Disease Control and Prevention, 1600 Clifton Rd NE, Mailstop H18-SB, Atlanta, GA 30329, USA.
Email: ocr3@cdc.gov

Review Editor: Alberto Diaspro

Abstract

The identification of viral particles within a tissue specimen requires specific knowledge of viral ultrastructure and replication, as well as a thorough familiarity with normal subcellular organelles. The severe acute respiratory syndrome coronavirus 2 (SARS-CoV-2) pandemic has underscored how challenging the task of identifying coronavirus by electron microscopy (EM) can be. Numerous articles have been published mischaracterizing common subcellular structures, including clathrin- or coatomer- coated vesicles, multivesicular bodies, and rough endoplasmic reticulum, as coronavirus particles in SARS-CoV-2 positive patient tissue specimens. To counter these misinterpretations, we describe the morphological features of coronaviruses that should be used to differentiate coronavirus particles from subcellular structures. Further, as many of the misidentifications of coronavirus particles have stemmed from attempts to attribute tissue damage to direct infection by SARS-CoV-2, we review articles describing ultrastructural changes observed in specimens from SARS-CoV-2-infected individuals that do not necessarily provide EM evidence of direct viral infection. Ultrastructural changes have been observed in respiratory, cardiac, kidney, and intestinal tissues, highlighting the widespread effects that SARS-CoV-2 infection may have on the body, whether through direct viral infection or mediated by SARS-CoV-2 infection-induced inflammatory and immune processes.

Highlights

The identification of coronavirus particles in SARS-CoV-2 positive tissues continues to be a challenging task. This review provides examples of coronavirus ultrastructure to aid in the differentiation of the virus from common cellular structures.

KEYWORDS
coronavirus, COVID-19, electron microscopy, SARS, SARS-CoV-2, ultrastructure

1 | INTRODUCTION

The coronavirus disease (COVID-19) pandemic has resulted in a renewed focus on transmission electron microscopy (EM) as a means of detecting viral particles within clinical and autopsy specimens. While the use of EM as a first-line diagnostic method in infectious disease has waned due to the advent of molecular techniques, EM continues to be an important tool for diagnosis and research into the ultrastructural basis of disease. It is particularly useful when the infectious agent is unknown and has not been detected by molecular or immunological techniques due to test specificity and sensitivity or reagent choice. For example, EM played a key role in the identification of a coronavirus as the causative agent of the 2002–2003 severe acute respiratory syndrome outbreak (Ksiazek et al., 2003). During the

COVID-19 pandemic, EM has proven valuable in establishing the extent of direct viral infection in clinical specimens (Dittmayer et al., 2020; Martines et al., 2020; Meinhardt et al., 2020) as well as providing insights into the effects of SARS-CoV-2 infection on tissues throughout the body (Kudose et al., 2020; Sharma et al., 2020).

Since early 2020, EM has been used to attempt to find SARS-CoV-2 particles in patient tissue specimens. Unfortunately, many of these studies have misidentified common subcellular structures as coronavirus particles, leading to confusion and the publication of inaccurate information. This is most problematic when EM is the only method used to detect a virus in a particular tissue or when all other diagnostic methods have yielded negative results. Numerous articles and letters to the editor have been written to address this ever-growing problem (Akilesh, Nicosia, et al., 2021; Bullock, Goldsmith, & Miller, 2021; Bullock, Goldsmith, Zaki, et al., 2021; Calomeni et al., 2020; Dittmayer et al., 2020; Goldsmith et al., 2020; Kniss, 2020; Miller & Brealey, 2020; Miller & Goldsmith, 2020; Neil et al., 2020; Roufosse et al., 2020). Additionally, more clinical and research articles are now providing examples of structures observed by EM in SARS-CoV-2 positive tissues that simply mimic viral particles (e.g., coated vesicles and multivesicular bodies) (Calabrese et al., 2020; Sharma et al., 2020).

With the aim of increasing accurate identification of coronavirus particles in COVID-19 cases, we provide herein examples of coronavirus particles as well as common subcellular structures that may be mistaken for viral particles. We also discuss complementary methods for virus identification to support traditional EM data and review studies reporting the ultrastructural pathology of SARS-CoV-2 infection.

2 | ANATOMY OF A CORONAVIRUS

Members of the family *Coronaviridae* all have the same morphology (Figure 1) (Almeida & Tyrrell, 1967; Goldsmith et al., 2004; Oshiro et al., 1971). The following morphologic characteristics must be present to conclusively identify suspected viral particles as coronavirus: 1) Coronaviruses are enveloped viruses that range in size from 60 nm to 140 nm in diameter. 2) Coronaviruses have surface peplomers (spikes) that may be visible on extracellular viral particles in thin section preparations (tissue specimens embedded in epoxy resin). Intracellular viral particles rarely have visible surface peplomers. The surface peplomers are most clearly visible in negative stain preparations (liquid samples stained with a heavy metal salt solution) (Hayat, 2000). 3) Intracellular viral particles are always contained within cytoplasmic vacuoles. 4) Coronaviruses have a helical nucleocapsid that is visible in cross section as small electron-dense dots that are 6–12 nm in diameter (Figure 1).

In addition to viral morphologic appearance, knowledge of the viral replicative process is also essential in correctly identifying a coronavirus. All coronaviruses mature by budding through the membranes

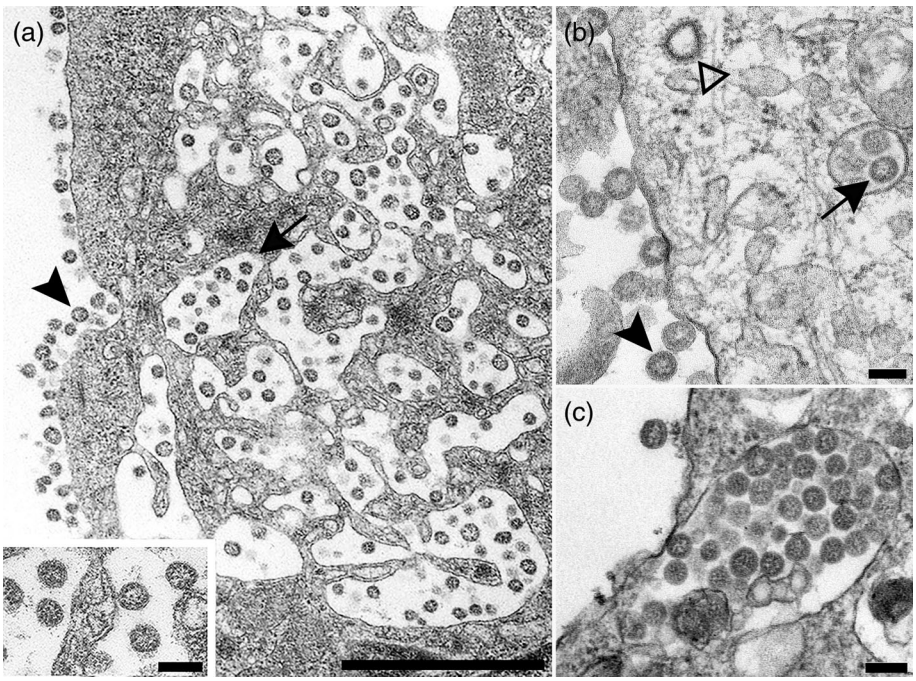

FIGURE 1 Electron microscopic images of three isolates of different members of the family *Coronaviridae* that have caused serious disease in recent years. (a) Severe acute respiratory syndrome coronavirus 1 (SARS-CoV-1) from 2002–2003. Intracellular viral particles are held within membrane-bound vacuoles (arrow), and extracellular viral particles line the cell surface (arrowhead). Scale bar: 1 μm. Inset: Higher magnification of SARS-CoV-1 particles. Scale bar: 100 nm. (b) Intracellular (arrow) and extracellular (closed arrowhead) accumulations of Middle East respiratory syndrome coronavirus (MERS-CoV). A clathrin-coated vesicle, often misidentified as coronavirus, is also visible free in the cytoplasm (open arrowhead). Scale bar: 100 nm. (c) Severe acute respiratory syndrome coronavirus −2 (SARS-CoV-2) from 2020. Vacuole containing SARS-CoV-2 particles fused to the plasma membrane of an infected cell. Scale bar: 100 nm

of the endoplasmic reticulum-Golgi complex, forming membrane-bound vacuoles containing viral particles within the intracisternal space (Goldsmith et al., 2004; Oshiro et al., 1971). Virions are then released from the cell by exocytosis once the viral vacuole fuses with the host cell plasma membrane (Figure 1c). Virus particles may stay attached to the cell surface. The attachment of the mature particles to the plasma membrane is a hallmark characteristic of coronaviruses (Figure 1a); however, this does not preclude the release of viral particles away from the infected cell. Coronavirus replication may also result in the formation of modified host cell membranes such as double-membrane vesicles and convoluted membranes, though these structures are not always observed in an infected cell (Knoops et al., 2008; Snijder et al., 2020). Because of the mechanism of coronavirus replication, coronavirus particles will not be found free in the cytoplasm, but instead will be held within membrane-bound vacuoles. Details of coronavirus morphology and replication should be used as a guide while attempting to identify the virus within an infected cell.

When analyzing autopsy tissues or formalin-fixed, paraffin-embedded (FFPE) tissues, the morphologic characteristics of coronaviruses may be difficult to perceive due to tissue autolysis and/or the additional processing that FFPE tissues undergo prior to being prepared for EM (Figure 2). In these cases, it is advisable to use additional diagnostic methods, such as immunohistochemistry (IHC) or in situ hybridization (ISH), to demonstrate the presence of the virus in tissue. For comparison, Figure 1 shows cell culture-grown isolates of coronaviruses held within membrane-bound vacuoles with visible cross sections through the nucleocapsids, while Figure 2 shows coronaviruses from formalin-fixed and FFPE autopsy tissues. In well preserved autopsy tissues, coronavirus particles are easily identifiable based on the morphologic features described above (Figure 2a). By contrast, viral particles from FFPE autopsy tissues are generally smaller in size due to shrinkage from processing and darker in appearance, making the cross sections through the nucleocapsids more difficult to see, and they may be less well defined (Figures 2b,c). The membranes of vacuolar accumulations of coronavirus particles are also not as well defined as those in cell culture specimens but are still visible (Figure 2b,c).

3 | CORONAVIRUS MISIDENTIFICATIONS

The misidentification of common subcellular structures as coronavirus in patient and autopsy tissue specimens has been a prevalent problem since the beginning of the COVID-19 pandemic. Between March 2020 and October 2021, at least 53 publications (Supplement) have incorrectly identified host cell structures as virus. Though far less frequent, examples of misidentified coronavirus can be found from the 2003 SARS-CoV-1 outbreak as well as from the 2012 MERS-CoV outbreak (Alsaad et al., 2018; Ding et al., 2004). Misidentifications of SARS-CoV-2 particles have occurred in nearly every tissue of the body (Table 1), leading to possible confusion as to whether the virus itself is causing tissue damage throughout the body or if tissue damage is a result of other factors, like the cytokine storm or downstream

TABLE 1 Misidentifications of SARS-CoV-2 by tissue type as of October 2021

Tissue	No. of publications
Lung	13
Kidney	12
Heart	9
Placenta	9
Intestine	5
Liver	5
Skin	3
Brain	2
Penis/Testis	2
Skeletal muscle	1
Salivary gland	1
Lymph nodes	1
Olfactory	1
Retina	1
Esophagus	1
Fetal tissue	1

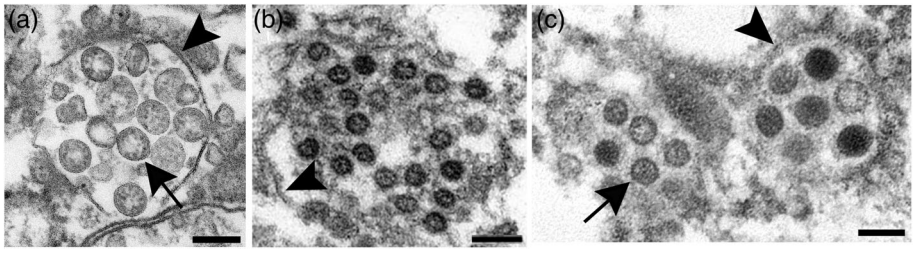

FIGURE 2 Coronaviruses detected in autopsy tissues. (a) Intracellular SARS-CoV-2 particles within a type II pneumocyte from well preserved autopsy tissue. The vacuolar membrane is clearly visible (arrowhead) as are the cross sections through the viral nucleocapsids (arrow). Scale bar: 100 nm. (b) Intracellular SARS-CoV-1 particles within a pneumocyte from formalin-fixed, paraffin-embedded (FFPE) autopsy tissue. Overall ultrastructure is deteriorated with viral particles appearing smaller than normal and more electron dense. The vacuolar membrane is visible (arrowhead) but appears less contiguous. Scale bar: 100 nm. Image reproduced from Shieh et al. (2005). (c) MERS-CoV particles in a deteriorating cell within the lung from FFPE autopsy tissue. Portions of the vacuolar membrane are visible (arrowhead) as are cross sections through the viral nucleocapsid on some viral particles (arrow). Image courtesy of Maureen Metcalfe, CDC. Scale bar: 100 nm

complications due to lack of proper function of an infected organ (Buja & Stone, 2021; Gustine & Jones, 2021; Perico et al., 2021). To date, SARS-CoV-2 particles have been correctly identified by EM only in the lung, heart, olfactory mucosa, and placenta (Birkhead et al., 2021; Dittmayer et al., 2020; Martines et al., 2020; Meinhardt et al., 2020; Nardacci et al., 2021; Reagan-Steiner et al., 2022). Dittmayer et al. (2020), Martines et al. (2020), and Meinhardt et al. (2020) provide the clearest examples of SARS-CoV-2 particles directly in infected tissues and also provide further correlation of their EM findings with other in situ SARS-CoV-2 detection methods, such as IHC assays. The limited number of tissues in which the virus has been correctly identified stands in stark contrast to the number of tissues in which the virus has been incorrectly identified, which includes lung, kidney, placenta, heart, liver, intestine, skin, testis, penis, and brain (Table 1). Letters to the Editor and review articles have attempted to address this ongoing issue, providing excellent examples of coronavirus and normal cellular ultrastructure (Akilesh, Nicosia, et al., 2021; Bullock, Goldsmith, & Miller, 2021; Bullock, Goldsmith, Zaki, et al., 2021; Calomeni et al., 2020; Dittmayer et al., 2020; Goldsmith et al., 2020; Kniss, 2020; Miller & Brealey, 2020; Miller & Goldsmith, 2020; Neil et al., 2020; Reagan-Steiner et al., 2022; Roufosse et al., 2020).

The subcellular structures misidentified as coronavirus have remained consistent, with the most mistaken structures being clathrin- or coatomer-coated vesicles (CCVs), multivesicular bodies (MVBs), and circular cross sections through the rough endoplasmic reticulum (RER) (Figure 1b-CCVs, Figure 3). By following the coronavirus identification criteria described above, one can easily differentiate a coronavirus particle from these more common cellular organelles (Bullock, Goldsmith, & Miller, 2021; Bullock, Goldsmith, Zaki, et al., 2021). CCVs, MVBs, and RER all lack the internal electron-dense black dots that signify cross-sections through the helical nucleocapsid curled up within the virus particle. While CCVs have a generally spherical shape and a fringe of spike-like clathrin or coatomer protein surrounding the vesicle, CCVs are found free in the cytoplasm, unlike coronaviruses which are found within membrane-bound vacuoles (Figure 1b, Figure 3a). The ribosomes along circular cross-sections through the RER may also have a spike-like appearance, but again, these structures are found free within the cytoplasm and vary more greatly in size than coronavirus particles (Figure 3b). MVBs are membrane-bound but do not contain the dense dots created by cross sections through the spiral-shaped, filamentous nucleocapsid that would be characteristic of a coronavirus (Figure 3c). Additionally, since coronaviruses typically are present as large accumulations of virions, finding just a single "particle" in a cell would be an indication that it most likely is not a coronavirus. All these characteristics should be kept in mind when attempting to differentiate a coronavirus from other structures within a cell. Additionally, many published EM images purporting to show coronavirus include structures that are entirely unidentifiable due to the quality of the tissue. Successful identification and differentiation of viral particles from other structures requires a certain level of ultrastructural preservation which may not be possible in some tissues due to autolysis or extensive tissue processing.

4 | COMPLEMENTARY METHODS FOR VIRUS DETECTION

EM evidence of viral infection in tissue specimens should be supported by additional methods of virus detection. IHC, ISH, and RT-PCR are all able to help build a strong case for the presence of an infectious agent, like coronavirus, within a tissue specimen. Further, IHC and ISH can help to guide the search for coronavirus by EM either through using FFPE samples for EM that have already tested positive for the virus or by indicating which types of cells show positive staining (Martines et al., 2020; Meinhardt et al., 2020; Ng et al., 2016; Shieh et al., 2005). Importantly, if the virus is not present in high enough numbers to be detected by PCR, IHC, ISH, or other sensitive methods, then the virus is unlikely to be visualizable using EM. In situ techniques, like ISH and IHC, have been used successfully to detect SARS-CoV-2 proteins and RNA in tissue specimens (Bhatnagar et al., 2021; Borczuk et al., 2020; Bradley et al., 2020; Martines et al., 2020; Meinhardt et al., 2020). These techniques provide valuable information regarding SARS-CoV-2 localization and, in the case of ISH, where the virus may be actively replicating. Additionally, ISH and IHC enable visualization of significantly larger areas of tissue than EM, allowing for a more widespread analysis of the effects of infection on tissue specimens. Multiple diagnostic methods should be used to complement and verify results across several testing platforms and to create a complete picture of the extent of infection.

An additional EM-based technique for detecting virus is immunoelectron microscopy (IEM), which uses immunogold to label viral particles and may be used to support traditional EM findings. One way to perform IEM is by omitting osmium staining and embedding infected

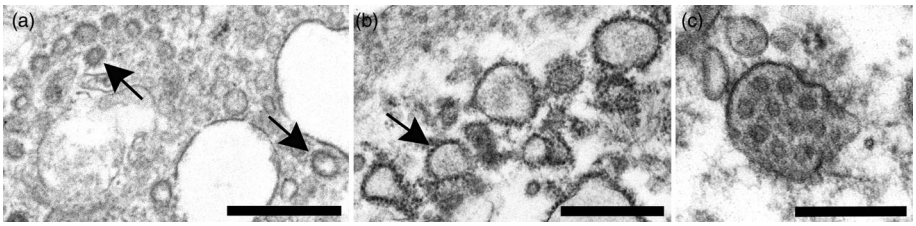

FIGURE 3 Subcellular structures commonly misidentified as coronavirus. (a) Clathrin-coated vesicles (CCVs; arrows). Scale bar: 500 nm. (b) Circular cross sections through rough endoplasmic reticulum (RER; arrow). Scale bar: 500 nm. (c) Multivesicular body (MVB). Scale bar: 250 nm

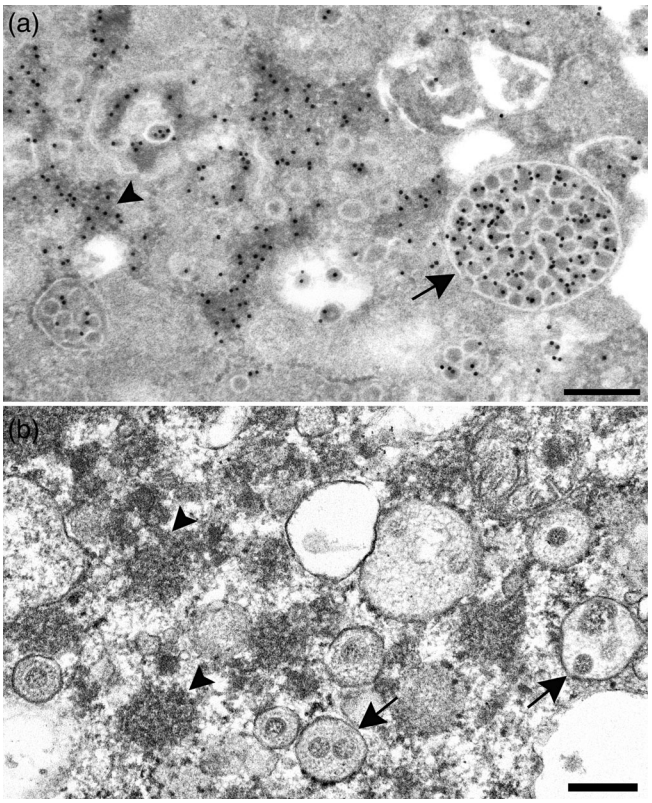

FIGURE 4 Immuno-electron microscopy (IEM) for SARS-CoV-2 using hyperimmune mouse ascites fluid raised against SARS-CoV-1. (a) IEM of SARS-CoV-2 infected cell culture embedded in LR white resin without osmification. Colloidal gold (electron dense, 12 nm black dots) identifies areas immunoreactive with the SARS-CoV-1 antibody, including vacuolar accumulations of presumed viral particles (arrow) and nucleocapsid inclusions (arrowhead). Scale bar: 200 nm. (b) SARS-CoV-2 infected cell culture osmicated and embedded using epoxy resin. The ultrastructure of the infected cell, vacuolar accumulation of coronavirus (arrows), and viral nucleocapsid inclusions (arrowheads) are more clearly defined than in the LR white embedded sample. Scale bar: 200 nm

cells in an acrylic resin (e.g., LR White, Electron Microscopy Sciences, Hatfield, PA), which is somewhat more porous than the routine EM epoxy (Goldsmith et al., 2003). A SARS-coronavirus specific antibody is applied to a thin section, followed by a secondary antibody conjugated to colloidal gold particles. The gold particles appear as electron dense black dots in areas where coronavirus is present or where the protein that the primary antibody targets is present, such as nucleocapsid inclusions (Figure 4a, cell culture). Due to the embedding technique used for IEM (the lack of osmification, as osmium would inactivate the immunological recognition of the antigen), the ultrastructure is less well defined than in a traditionally embedded EM sample. In Figure 4a, spherical structures consistent in size with coronavirus and in membrane-bound vacuoles are labeled with colloidal gold as are more electron dense areas of the cytoplasm that are likely nucleocapsid inclusions. For comparison, Figure 4b shows an area of a traditionally embedded and osmicated EM specimen that contains many of the same viral features as Figure 4a, that is, vacuolar accumulations of coronavirus particles and nucleocapsid inclusions in the cytoplasm. While the same FFPE block can be used for IHC, ISH, and EM, the embedding technique used for IEM requires that a different wet tissue specimen be selected for this process. As such, it is not possible to examine by IEM the exact same FFPE tissue found positive by light microscopy. Other methods for IEM exist, including ultrathin cryosections, which expose viral antigens, but this method requires special tissue preparation and also produces a result that requires practiced interpretation since the ultrastructural appearance differs from the conventional EM appearance. Grootemaat et al. have elegantly used this technique to demonstrate antigens of coronavirus grown in tissue culture (Grootemaat et al., 2022). Despite these limitations, IEM can still be a valuable tool to confirm the presence of a virus in cells.

5 | ULTRASTRUCTURAL CHANGES CAUSED BY SARS-COV-2 INFECTION

An increasing number of articles have included descriptions of ultrastructural changes in SARS-CoV-2 positive autopsy tissues (Ackermann et al., 2020; Akilesh, Nast, et al., 2021; Deinhardt-Emmer, Böttcher, et al., 2021; Deinhardt-Emmer, Wittschieber, et al., 2021; Duarte-Neto et al., 2021; Lüke et al., 2020; Rizzo et al., 2021; Santana et al., 2021; Saraiva et al., 2021). These articles do not necessarily include EM images of viral particles but describe possible ultrastructural alterations due to infection. Bear in mind that some ultrastructural changes may be due to or impacted by co-morbidities and/or tissue autolysis, rather than exclusively a result of viral infection. Comparison of infected and healthy tissues is necessary, and correlation with results of other diagnostic techniques is always recommended. Respiratory system changes due to SARS-CoV-2 infection have been most thoroughly described (Ackermann et al., 2020; Martines et al., 2020; Santana et al., 2021; Saraiva et al., 2021). Type I pneumocyte degeneration, type II pneumocyte hyperplasia, and hyaline membrane formation were common ultrastructural features of SARS-CoV-2 infection (Martines et al., 2020; Santana et al., 2021). A recent study of nasopharyngeal epithelial cells from SARS-CoV-2 infected individuals showed loss of microvilli and the primary cilium in squamous cells as well as an increase in the number of multivesicular bodies and autophagosomes when compared with specimens from SARS-CoV-2 negative individuals (Saraiva et al., 2021). Santana et al. further noted disruption of the epithelial-endothelial barrier, in addition to cellular debris and fibrin in the alveolar space and detachment of type II pneumocytes from the basement membrane (Santana et al., 2021). Observations of vessel barrier damage are in agreement with suggestions that these changes and increases in pro-inflammatory cytokines contribute to the development of acute respiratory distress syndrome in COVID-19 patients by mediating inflammatory cell infiltration in the lungs (Perico et al., 2021).

Multiple studies have observed that endothelial dysfunction is a common occurrence in patients with severe COVID-19. Much of this endothelial dysfunction involves vascular inflammation as well as

perivascular T-cell recruitment that results in disruption of the alveolar-capillary barrier and increased barrier permeability. Endothelial dysfunction has been demonstrated in autopsy tissue specimens as well as in cell culture systems designed to model the alveolar-capillary barrier (Ackermann et al., 2020; Deinhardt-Emmer, Böttcher, et al., 2021; Deinhardt-Emmer, Wittschieber, et al., 2021; Santana et al., 2021). A study by Ackerman et al., comparing lung tissues from patients who died from COVID-19 to those that had died from influenza, demonstrated that more microthrombi were observed in SARS-CoV-2 infected lungs. These researchers also observed intussusceptive angiogenesis both in early and in prolonged SARS-CoV-2 lung infection, and EM showed the formation of intussusceptive pillars and distorted vessels with ruptured endothelial cells in the alveolar septum (Ackermann et al., 2020; Duarte-Neto et al., 2021). Within cardiac tissue, disrupted endothelial cells resulting in direct contact of myocardial cells with the vascular lumen were noted in severe COVID-19 cases (Duarte-Neto et al., 2021). Recent reviews of clinical and autopsy studies from 2020 indicate that endothelial dysfunction during SARS-CoV-2 infection, such as those seen by EM, are key to inciting the inflammatory processes that cause more severe COVID-19 (Buja & Stone, 2021; Perico et al., 2021).

Endothelial injury and acute kidney injury have been described in kidney biopsy and autopsy specimens from SARS-CoV-2 positive patients. Ultrastructural changes include widening of the glomerular subendothelial space, acute tubular necrosis, and diffuse podocyte foot-process effacement (Akilesh, Nast, et al., 2021; Sharma et al., 2020). In cases of more severe kidney injury, there was evidence of endothelial cell swelling and fibrin thrombi within glomerular hilar arterioles. To date, no coronavirus particles have been found in the kidney to suggest that kidney injury is due to direct infection. Kidney injury, like damage in other non-respiratory tissues, may be caused by cytokine-mediated effects and the inflammatory response as indicated by the elevated levels of serum cytokines and inflammatory markers in patients with severe COVID-19 (Doykov et al., 2020; Gustine & Jones, 2021; Kudose et al., 2020). Lastly, Rizzo et al., described ultrastructural changes to the microvilli of the intestine, noting areas of shortened and disorganized microvilli that corresponded to the site of a bleeding ulceration. These areas were also positive by IHC for SARS-CoV-2 nucleocapsid protein (Rizzo et al., 2021).

The ultrastructural changes observed throughout disparate organs highlight the effects that SARS-CoV-2 can have throughout the body, whether through direct viral infection or mediated by inflammatory and immune processes in other tissues. Importantly, the studies discussed above underscore how it is possible to visualize the ultrastructural damage due to SARS-CoV-2 infection without necessarily observing the virus itself by EM.

6 | CONCLUSION

The COVID-19 pandemic has brought into focus the importance of interdisciplinary collaborations to investigate all facets of disease pathology. Including EM in the investigative repertoire enables researchers to take a close look at the ultrastructural changes caused by viral infection and collect strong evidence of the presence of virus in a tissue. Identification of any virus by EM should be informed by knowledge of viral ultrastructure and replication as well as familiarity with subcellular ultrastructure (Ghadially, 1997; Haguenau & Dalton, 1973; Maunsbach & Afzelius, 1998). In the case of coronaviruses, intracellular viral particles will be held within membrane-bound vacuoles, and extracellular particles will likely cluster along the outside of the infected cell and may or may not have visible spikes. The coronavirus particles will be 60 nm to 140 nm in diameter and will show multiple electron dense cross sections through the helical viral nucleocapsid. Successful identification of a coronavirus in infected tissue requires all these morphologic criteria to be present. Employing multiple methods of viral detection, including IHC, ISH, PCR, and IEM, is always advisable for a more robust argument for the presence of a virus within a tissue specimen.

Combining ultrastructural study with molecular, chemical, histologic, and immunohistochemical data has enabled the building of a more complete picture of the scope of SARS-CoV-2 infection. Observations of ultrastructural damage have emphasized the extent to which COVID-19 is a systemic disease that can have manifestations throughout the body, affecting even organs and tissues not directly infected by SARS-CoV-2. By using EM as part of a multifaceted approach, we can provide accurate and valuable information concerning SARS-CoV-2 infection.

ACKNOWLEDGMENT

We thank Maureen Metcalfe for providing the image of MERS-CoV from autopsy tissue.

DISCLAIMER

The findings and conclusions in this report are those of the authors and do not necessarily represent the official position of the Centers for Disease Control and Prevention.

ORCID

Hannah A. Bullock https://orcid.org/0000-0002-4811-1274

REFERENCES

Ackermann, M., Mentzer, S. J., Kolb, M., & Jonigk, D. (2020). Inflammation and intussusceptive angiogenesis in COVID-19: Everything in and out of flow. *The European Respiratory Journal*, *56*(5), 2003147. https://doi.org/10.1183/13993003.03147-2020

Akilesh, S., Nast, C. C., Yamashita, M., Henriksen, K., Charu, V., Troxell, M. L., Kambham, N., Bracamonte, E., Houghton, D., Ahmed, N. I., Chong, C. C., Thajudeen, B., Rehman, S., Khoury, F., Zuckerman, J. E., Gitomer, J., Raguram, P. C., Mujeeb, S., Schwarze, U., … Smith, K. D. (2021). Multicenter clinicopathologic correlation of kidney biopsies performed in COVID-19 patients presenting with acute kidney injury or proteinuria. *American Journal of Kidney Diseases*, *77*(1), 82–93. https://doi.org/10.1053/j.ajkd.2020.10.001

Akilesh, S., Nicosia, R. F., Alpers, C. E., Tretiakova, M., Hsiang, T. Y., Gale, M., & Smith, K. D. (2021). Characterizing viral infection by electron microscopy: Lessons from the coronavirus disease 2019 pandemic. *The American Journal of Pathology*, *191*(2), 222–227. https://doi.org/10.1016/j.ajpath.2020.11.003

Almeida, J. D., & Tyrrell, D. A. (1967). The morphology of three previously uncharacterized human respiratory viruses that grow in organ culture. *The Journal of General Virology*, *1*(2), 175–178. https://doi.org/10.1099/0022-1317-1-2-175

Alsaad, K. O., Hajeer, A. H., Al Balwi, M., Al Moaiqel, M., Al Oudah, N., Al Ajlan, A., AlJohani, S., Alsolamy, S., Gmati, G. E., Balkhy, H., Al-Jahdali, H. H., Baharoon, S. A., & Arabi, Y. M. (2018). Histopathology of Middle East respiratory syndrome coronovirus (MERS-CoV) infection – Clinicopathological and ultrastructural study. *Histopathology*, *72*(3), 516–524. https://doi.org/10.1111/his.13379

Bhatnagar, J., Gary, J., Reagan-Steiner, S., Estetter, L. B., Tong, S., Tao, Y., Denison, A. M., Lee, E., DeLeon-Carnes, M., Li, Y., Uehara, A., Paden, C. R., Leitgeb, B., Uyeki, T. M., Martines, R. B., Ritter, J. M., Paddock, C. D., Shieh, W. J., & Zaki, S. R. (2021). Evidence of severe acute respiratory syndrome coronavirus 2 replication and tropism in the lungs, airways, and vascular endothelium of patients with fatal coronavirus disease 2019: An autopsy case series. *The Journal of Infectious Diseases*, *223*(5), 752–764. https://pubmed.ncbi.nlm.nih.gov/33502471/

Birkhead, M., Glass, A. J., Allan-Gould, H., Goossens, C., & Wright, C. A. (2021). Ultrastructural evidence for vertical transmission of SARS-CoV-2. *International Journal of Infectious Diseases*, *111*, 10–11. https://doi.org/10.1016/j.ijid.2021.08.020

Borczuk, A. C., Salvatore, S. P., Seshan, S. V., Patel, S. S., Bussel, J. B., Mostyka, M., Elsoukkary, S., He, B., del Vecchio, C., Fortarezza, F., Pezzuto, F., Navalesi, P., Crisanti, A., Fowkes, M. E., Bryce, C. H., Calabrese, F., & Beasley, M. B. (2020). COVID-19 pulmonary pathology: A multi-institutional autopsy cohort from Italy and New York City. *Modern Pathology*, *33*, 2156–2168. https://doi.org/10.1038/s41379-020-00661-1

Bradley, B. T., Maioli, H., Johnston, R., Chaudhry, I., Fink, S. L., Xu, H., Najafian, B., Deutsch, G., Lacy, J. M., Williams, T., Yarid, N., & Marshall, D. A. (2020). Histopathology and ultrastructural findings of fatal COVID-19 infections in Washington State: A case series. *Lancet*, *396*, 320–332. https://doi.org/10.1016/S0140-6736(20)31305-2

Buja, L. M., & Stone, J. R. (2021). A novel coronavirus meets the cardiovascular system: Society for Cardiovascular Pathology Symposium 2021. *Cardiovascular Pathology*, *53*, 107336. https://doi.org/10.1016/j.carpath.2021.107336

Bullock, H. A., Goldsmith, C. S., & Miller, S. E. (2021). Best practices for correctly identifying coronavirus by transmission electron microscopy. *Kidney International*, *99*(4), 824–827. https://doi.org/10.1016/j.kint.2021.01.004

Bullock, H. A., Goldsmith, C. S., Zaki, S. R., Martines, R. B., & Miller, S. E. (2021). Difficulties in differentiating coronaviruses from subcellular structures in human tissues by electron microscopy. *Emerging Infectious Diseases*, *27*(4), 1023–1031. https://doi.org/10.3201/eid2704.204337

Calabrese, F., Pezzuto, F., Fortarezza, F., Hofman, P., Kern, I., Panizo, A., von der Thüsen, J., Timofeev, S., Gorkiewicz, G., & Lunardi, F. (2020). Pulmonary pathology and COVID-19: Lessons from autopsy. The experience of European Pulmonary Pathologists. *Virchows Archiv*, *477*(3), 359–372. https://doi.org/10.1007/s00428-020-02886-6

Calomeni, E., Satoskar, A., Ayoub, I., Brodsky, S., Rovin, B. H., & Nadasdy, T. (2020). Multivesicular bodies mimicking SARS-CoV-2 in patients without COVID-19. *Kidney International*, *98*(1), 233–234. https://doi.org/10.1016/j.kint.2020.05.003

Deinhardt-Emmer, S., Böttcher, S., Häring, C., Giebeler, L., Henke, A., Zell, R., Jungwirth, J., Jordan, P. M., Werz, O., Hornung, F., Brandt, C., Marquet, M., Mosig, A. S., Pletz, M. W., Schacke, M., Rödel, J., Heller, R., Nietzsche, S., Löffler, B., & Ehrhardt, C. (2021). SARS-CoV-2 causes severe epithelial inflammation and barrier dysfunction. *Journal of Virology*, *95*(10), 110–121. https://doi.org/10.1128/JVI.00110-21

Deinhardt-Emmer, S., Wittschieber, D., Sanft, J., Kleemann, S., Elschner, S., Haupt, K. F., Vau, V., Häring, C., Rödel, J., Henke, A., Ehrhardt, C., Bauer, M., Philipp, M., Gaßler, N., Nietzsche, S., Löffler, B., & Mall, G. (2021). Early postmortem mapping of SARS-CoV-2 RNA in patients with covid-19 and the correlation with tissue damage. *eLife*, *10*, e60361. https://doi.org/10.7554/eLife.60361

Ding, Y., He, L., Zhang, Q., Huang, Z., Che, X., Hou, J., Wang, H., Shen, H., Qiu, L., Li, Z., Geng, J., Cai, J., Han, H., Li, X., Kang, W., Weng, D., Liang, P., & Jiang, S. (2004). Organ distribution of severe acute respiratory syndrome (SARS) associated coronavirus (SARS-CoV) in SARS patients: Implications for pathogenesis virus transmission pathways. *The Journal of Pathology*, *203*(2), 622–630. https://doi.org/10.1002/path.1560

Dittmayer, C., Meinhardt, J., Radbruch, H., Radke, J., Heppner, B. I., Heppner, F. L., Stenzel, W., Holland, G., & Laue, M. (2020). Why misinterpretation of electron micrographs in SARS-CoV-2-infected tissue goes viral. *Lancet*, *396*, e64–e65. https://doi.org/10.1016/S0140-6736(20)32079-1

Doykov, I., Hällqvist, J., Gilmour, K. C., Grandjean, L., Mills, K., & Heywood, W. E. (2020). 'The long tail of Covid-19' – The detection of a prolonged inflammatory response after a SARS-CoV-2 infection in asymptomatic and mildly affected patients. *F1000Research*, *9*(1349), 1–9. https://doi.org/10.12688/f1000research.27287.1

Duarte-Neto, A. N., Caldini, E. G., Gomes-Gouvêa, M. S., Kanamura, C. T., de Almeida Monteiro, R. A., Ferranti, J. F., Ventura, A. M. C., Regalio, F. A., Fiorenzano, D. M., Gibelli, M. A. B. C., Carvalho, W. B., Leal, G. N., Pinho, J. R. R., Delgado, A. F., Carneiro-Sampaio, M., Mauad, T., Ferraz da Silva, L. F., Saldiva, P. H. N., & Dolhnikoff, M. (2021). An autopsy study of the spectrum of severe COVID-19 in children: From SARS to different phenotypes of MIS-C. *EClinicalMedicin*, *35*, 100850. https://doi.org/10.1016/j.eclinm.2021.100850

Ghadially, F. (1997). Ultrastructural pathology of the cell and matrix. In *Ultrastructural pathology of the cell and matrix* (4th ed.). Butterworth-Heinemann.

Goldsmith, C. S., Miller, S. E., Martines, R. B., Bullock, H. A., & Zaki, S. R. (2020). Electron microscopy of SARS-CoV-2: A challenging task. *Lancet*, *395*, e99. https://doi.org/10.1016/S0140-6736(20)31188-0

Goldsmith, C. S., Tatti, K. M., Ksiazek, T. G., Rollin, P. E., Comer, J. A., Lee, W. W., Rota, P. A., Bankamp, B., Bellini, W. J., & Zaki, S. R. (2004). Ultrastructural characterization of SARS coronavirus. *Emerging Infectious Diseases*, *10*(2), 320–326. https://doi.org/10.3201/eid1002.030913

Goldsmith, C. S., Whistler, T., Rollin, P. E., Ksiazek, T. G., Rota, P. A., Bellini, W. J., Daszak, P., Wong, K. T., Shieh, W. J., & Zaki, S. R. (2003). Elucidation of Nipah virus morphogenesis and replication using ultrastructural and molecular approaches. *Virus Research*, *92*(1), 89–98. https://doi.org/10.1016/S0168-1702(02)00323-4

Grootemaat, A. E., van der Niet, S., Scholl, E. R., Roos, E., Schurink, B., Bugiani, M., Miller, S. E., Larsen, P., Pankras, J., Reits, E. A., & van der Wel, N. N. (2022). Lipid and nucleocapsid N-protein accumulation in COVID-19 patient lung and infected cells. *Microbiology Spectrum*, *10*(1), e01271–e01221. https://doi.org/10.1128/spectrum.01271-21

Gustine, J. N., & Jones, D. (2021). Immunopathology of hyperinflammation in COVID-19. *The American Journal of Pathology*, *191*(1), 4–17. https://doi.org/10.1016/j.ajpath.2020.08.009

Haguenau, F., & Dalton, D. (1973). In A. J. Dalton & F. Haguenau (Eds.), *Ultrastructure of animal viruses and bacteriophages: An atlas* (pp. 391–397). Academic Press, Inc.

Hayat, M. (2000). *Principles and techniques of electron microscopy: Biological applications* (4th ed., pp. 134–138). Cambridge University Press.

Kniss, D. A. (2020). Alternative interpretation to the findings reported in visualization of severe acute respiratory syndrome coronavirus 2 invading the human placenta using electron microscopy. *American Journal of Obstetrics and Gynecology*, *233*, 785–786. https://doi.org/10.1016/j.ajog.2020.06.016

Knoops, K., Kikkert, M., Van Den Worm, S. H. E., Zevenhoven-Dobbe, J. C., Van Der Meer, Y., Koster, A. J., Mommaas, A. M., & Snijder, E. J. (2008). SARS-coronavirus replication is supported by a

reticulovesicular network of modified endoplasmic reticulum. *PLoS Biology*, *6*(9), 1957–1974. https://doi.org/10.1371/journal.pbio.0060226

Ksiazek, T. G., Erdman, D., Goldsmith, C. S., Zaki, S. R., Peret, T., Emery, S., Tong, S., Urbani, C., Comer, J. A., Lim, W., Rollin, P. E., Dowell, S. F., Ling, A. E., Humphrey, C. D., Shieh, W. J., Guarner, J., Paddock, C. D., Rota, P., Fields, B., … the SARS Working Group. (2003). A novel coronavirus associated with severe acute respiratory syndrome. *The New England Journal of Medicine*, *348*(20), 1953–1966. https://doi.org/10.1056/NEJMoa030781

Kudose, S., Batal, I., Santoriello, D., Xu, K., Barasch, J., Peleg, Y., Canetta, P., Ratner, L. E., Marasa, M., Gharavi, A. G., Stokes, M. B., Markowitz, G. S., & D'Agati, V. D. (2020). Kidney biopsy findings in patients with COVID-19. *Journal of the American Society of Nephrology*, *31*(9), 1959–1968. https://doi.org/10.1681/ASN.2020060802

Lüke, F., Orsó, E., Kirsten, J., Poeck, H., Grube, M., Wolff, D., Burkhardt, R., Lunz, D., Lubnow, M., Schmidt, B., Hitzenbichler, F., Hanses, F., Salzberger, B., Evert, M., Herr, W., Brochhausen, C., Pukrop, T., Reichle, A., & Heudobler, D. (2020). Coronavirus disease 2019 induces multi-lineage, morphologic changes in peripheral blood cells. *eJHaem*, *1*(1), 376–383. https://doi.org/10.1002/jha2.44

Martines, R. B., Ritter, J. M., Matkovic, E., Gary, J., Bollweg, B. C., Bullock, H., Goldsmith, C. S., Silva-Flannery, L., Seixas, J. N., Reagan-Steiner, S., Uyeki, T., Denison, A., Bhatnagar, J., Shieh, W. J., Zaki, S. R., & COVID-19 Pathology Working Group. (2020). Pathology and pathogenesis of SARS-CoV-2 associated with fatal coronavirus disease, United States. *Emerging Infectious Diseases*, *26*(9), 2005–2015. https://doi.org/10.3201/eid2609.202095

Maunsbach, A. B., & Afzelius, B. (1998). *Biomedical electron microscopy: Illustrated methods and interpretations*. Academic Press.

Meinhardt, J., Radke, J., Dittmayer, C., Franz, J., Thomas, C., Mothes, R., Laue, M., Schneider, J., Brünink, S., Greuel, S., Lehmann, M., Hassan, O., Aschman, T., Schumann, E., Chua, R. L., Conrad, C., Eils, R., Stenzel, W., Windgassen, M., … Heppner, F. L. (2020). Olfactory transmucosal SARS-CoV-2 invasion as a port of central nervous system entry in individuals with COVID-19. *Nature Neuroscience*, *24*, 168–175. https://doi.org/10.1038/s41593-020-00758-5

Miller, S. E., & Brealey, J. K. (2020). Visualization of putative coronavirus in kidney. *Kidney International*, *98*, 231–232. https://doi.org/10.1016/j.kint.2020.05.004

Miller, S. E., & Goldsmith, C. S. (2020). Caution in identifying coronaviruses by electron microscopy. *Journal of the American Society of Nephrology*, *31*, 2223–2224. https://doi.org/10.1681/ASN.2020050755

Nardacci, R., Colavita, F., Castilletti, C., Lapa, D., Matusali, G., Meschi, S., del Nonno, F., Colombo, D., Capobianchi, M. R., Zumla, A., Ippolito, G., Piacentini, M., & Falasca, L. (2021). Evidences for lipid involvement in SARS-CoV-2 cytopathogenesis. *Cell Death & Disease*, *12*(3), 1–12. https://doi.org/10.1038/s41419-021-03527-9

Neil, D., Moran, L., Horsfield, C., Curtis, E., Swann, O., Barclay, W., Hanley, B., Hollinshead, M., & Roufosse, C. (2020). Ultrastructure of cell trafficking pathways and coronavirus: How to recognise the wolf amongst the sheep. *The Journal of Pathology*, *252*(4), 346–357. https://doi.org/10.1002/path.5547

Ng, D. L., Al Hosani, F., Keating, M. K., Gerber, S. I., Jones, T. L., Metcalfe, M. G., Tong, S., Tao, Y., Alami, N. N., Haynes, L. M., Mutei, M. A., Abdel-Wareth, L., Uyeki, T. M., Swerdlow, D. L., Barakat, M., & Zaki, S. R. (2016). Clinicopathologic, immunohistochemical, and ultrastructural findings of a fatal case of middle east respiratory syndrome coronavirus infection in The United Arab Emirates, April 2014. *The American Journal of Pathology*, *186*(3), 652–658. https://doi.org/10.1016/j.ajpath.2015.10.024

Oshiro, L., Schieble, J., & Lennette, E. (1971). Electron microscopic studies of corornavirus. *The Journal of General Virology*, *12*(3), 161–168. https://doi.org/10.1099/0022-1317-12-2-161

Perico, L., Benigni, A., Casiraghi, F., Ng, L. F. P., Renia, L., & Remuzzi, G. (2021). Immunity, endothelial injury and complement-induced coagulopathy in COVID-19. *Nature Reviews Nephrology*, *17*(1), 46–64. https://doi.org/10.1038/s41581-020-00357-4

Reagan-Steiner, S., Bhatnagar, J., Martines, R. B., Milligan, N. S., Gisondo, C., Williams, F. B., Lee, E., Estetter, L., Bullock, H., Goldsmith, C. S., Fair, P., Hand, J., Richardson, G., Woodworth, K. R., Oduyebo, T., Galang, R. R., Phillips, R., Belyaeva, E., Yin, X. M., … Zaki, S. R. (2022). Detection of SARS-CoV-2 in neonatal autopsy tissues and placenta. *Emerging Infectious Diseases*, *28*(3), 510–517. https://wwwnc.cdc.gov/eid/article/28/3/21-1735_article

Rizzo, R., Neri, L. M., Simioni, C., Bortolotti, D., Occhionorelli, S., Zauli, G., Secchiero, P., Semprini, C. M., Laface, I., Sanz, J. M., Lanza, G., Gafà, R., & Passaro, A. (2021). SARS-CoV-2 nucleocapsid protein and ultrastructural modifications in small bowel of a 4-week-negative COVID-19 patient. *Clinical Microbiology and Infection*, *27*(6), 936–937. https://doi.org/10.1016/j.cmi.2021.01.012

Roufosse, C., Curtis, E., Moran, L., Hollinshead, M., Cook, T., Hanley, B., Horsfield, C., & Neil, D. (2020). Electron microscopic investigations in COVID-19: Not all crowns are coronas. *Kidney International*, *98*(2), 505–506. https://doi.org/10.1016/j.kint.2020.05.012

Santana, M. F., Pinto, R. A. d. A., Marcon, B. H., de Medeiros, L. C. A. S., de Morais, T. B. d. N., Dias, L. C., de Souza, L. P., de Melo, G. C., Monteiro, W. M., Lacerda, M. V. G., Val, F. A., Lalwani, P. J., & de Lima Ferreira, L. C. (2021). Pathological findings and morphologic correlation of the lungs of autopsied patients with SARS-CoV-2 infection in the Brazilian Amazon using transmission electron microscopy. *Revista da Sociedade Brasileira de Medicina Tropical*, *54*, 850–2020. https://doi.org/10.1590/0037-8682-0850-2020

Saraiva, K. L. A., Vasconcelos, L. R. S., Filgueira Bezerra, M., Arcoverde, R. M. L., Pinto Brandão-Filho, S., Ayres, C. F. J., de Figueiredo, R. C. B. Q., & Pereira-Neves, A. (2021). Ultrastructural analysis of nasopharyngeal epithelial cells from patients with SARS-CoV-2 infection. *BioRxiv Preprint*, 1–23. https://doi.org/10.1101/2021.07.08.451607

Sharma, P., Uppal, N. N., Wanchoo, R., Shah, H. H., Yang, Y., Parikh, R., Khanin, Y., Madireddy, V., Larsen, C. P., Jhaveri, K. D., Bijol, V., & Northwell Nephrology COVID-19 Research Consortium. (2020). COVID-19-associated kidney injury: A case series of kidney biopsy findings. *Journal of the American Society of Nephrology*, *31*, 1948–1958. https://doi.org/10.1681/ASN.2020050699

Shieh, W. J., Hsiao, C. H., Paddock, C. D., Guarner, J., Goldsmith, C. S., Tatti, K., Packard, M., Mueller, L., Wu, M. Z., Rollin, P., Su, I. J., & Zaki, S. R. (2005). Immunohistochemical, in situ hybridization, and ultrastructural localization of SARS-associated coronavirus in lung of a fatal case of severe acute respiratory syndrome in Taiwan. *Human Pathology*, *36*(3), 303–309. https://doi.org/10.1016/j.humpath.2004.11.006

Snijder, E. J., Limpens, R. W. A. L., de Wilde, A. H., de Jong, A. W. M., Zevenhoven-Dobbe, J. C., Maier, H. J., Faas, F. F. G. A., Koster, A. J., & Bárcena, M. (2020). A unifying structural and functional model of the coronavirus replication organelle: Tracking down RNA synthesis. *PLoS Biology*, *18*(6), 1–25. https://doi.org/10.1371/journal.pbio.3000715

SUPPORTING INFORMATION

Additional supporting information may be found in the online version of the article at the publisher's website.

How to cite this article: Bullock, H. A., Goldsmith, C. S., & Miller, S. E. (2022). Detection and identification of coronaviruses in human tissues using electron microscopy. *Microscopy Research and Technique*, *85*(7), 2740–2747. https://doi.org/10.1002/jemt.24115